J. Fluid Mech. (1976), *vol.* 74, *part* 3, *pp.* 547–560
Printed in Great Britain

Intrusion into a stratified fluid

By P. C. MANINS

CSIRO Division of Atmospheric Physics, P.O. Box 77, Mordialloc, Victoria 3195, Australia

(Received 12 August 1975)

Preliminary measurements have been made of the debouching of homogeneous fluid from a broad source at its equilibrium depth into a linearly stratified tank of salt water. With c the velocity of the nose of the intrusion, h its half-thickness near the source, N the environmental buoyancy frequency and ν the kinematic viscosity of the fluid, it is shown for $100 \lesssim Re \equiv 2ch/\nu \lesssim 500$ that the intrusion becomes practically steady under an inertia–buoyancy balance. The internal Froude number $Fr \equiv c/Nh$ is shown to be of order unity. Forward-propagating disturbances and the ends of the tank are inferred to play an important part in the flow.

1. Introduction

Having risen as high as its momentum and buoyancy will carry it, a buoyant plume in a stably stratified environment settles at its equilibrium (or neutral buoyancy) level and spreads horizontally. It is the behaviour of an idealized spreading front, or 'intrusion', which is studied in the laboratory experiments reported here.

Such intrusions are characterized by the following salient features.

(i) A stratified environment which may or may not be bounded in vertical or horizontal extent.

(ii) The intruding fluid is practically homogeneous, discharging at its equilibrium level under gravity.

(iii) The thickness and velocity of the intrusion are not primarily controlled by imposed boundary conditions except in so far as the volume flux of fluid is specified. Rather, the flow is dynamically self-determined.

(iv) The Reynolds number based on intrusion volume flux is generally much greater than unity. Thus at least in the initial stages of horizontal spreading viscous stresses ought to be relatively unimportant.

The emphasis of the preliminary laboratory experiments presented was on an approximately two-dimensional realization of the intrusion itself: the concomitant response of the stratified environment was not studied in detail. Further, the geometry of the source of the intruding fluid was carefully chosen so as to obviate entrainment of ambient fluid and permit study of the dynamics of the intrusion. The Reynolds number of the intrusions was made as large as was practical (up to 540 based on total volume flux per unit breadth from the source)

so that viscous effects were minimized, but not so large that the flow resulted in turbulent entrainment. It follows that the range of conditions was quite limited. Solutions of salt in water were used so the Prandtl number $\sigma \equiv \nu/\kappa$ was large (about 300). Here ν and κ are the kinematic viscosity and diffusivity of salt respectively for water.

Since the problem of a rapid intrusion into a stably stratified fluid is the analogue of a gravity current in homogeneous fluid, it may be anticipated that the internal Froude number $Fr \equiv c/Nh$ is of order unity, expressing a balance between inertia and buoyancy forces. Here c and h are a characteristic velocity and thickness of the intrusion, and N is the environmental buoyancy frequency.

Thus, in summary, the parameter regime for the experiments described here is

$$Re \gg 1, \quad Fr \sim 1, \quad \sigma \gg 1.$$

2. Experiment arrangement

The experiments were conducted in a tank (183 cm long × 10·3 cm broad × 20 cm deep) filled with linearly stratified salt water to a depth of 13–16 cm. This was prepared by a variant of the 'pile-on' two-tank method due to Fortuin (1960). Installed vertically at one end of the tank was a rectangular tube 24 cm high, of the same breadth as the tank, and blocked off at the lower end only. A strip 3 cm deep on one face adjacent to this end was cut away over the full breadth and covered in steel gauze and expanded PVC so as to act as a deep-mouthed two-dimensional source of homogeneous intrusion fluid. The source supply was via a constant-head tank and flowmeter. These arrangements ensured that the volume flux through the source was constant: the fluid depth in the source tube adjusted itself rapidly to supply the necessary total head at any instant. Just before a run was begun 1 ml samples of the stratified fluid were withdrawn at 2 cm vertical intervals, sampling simultaneously. The samples' refractive indices were determined to check the linearity of the stratification and to set the density of the source fluid so as it had an equilibrium depth of half the working depth in the tank.

Data were obtained from a sequence of photographs of a simple shadowgraph. This was formed by illuminating a sheet of tracing paper on the front of the tank through the working fluid by a QI light source situated 4 m behind the tank. In some experiments vertical density profiles were obtained before and during the run by traversing a point conductivity probe of design similar to that described by Mied & Merceret (1968). In yet fewer experiments velocity profiles were measured by observing the time-distortion of traces left by dropping potassium permanganate crystals into the tank.

3. Background

The problem of the establishment of a discharge into a stratified fluid has received little attention so far. Indeed, almost all theoretical understanding is by implication from studies of obstacles moving transversely in stratified fluid of infinite lateral extent at low Reynolds number and low internal Froude number.

Browand & Winant (1972) extended Graebel's (1969) theoretical treatment of obstacles valid for non-diffusive fluids such that

$$Fr^2 \ll 1, \quad Re/Fr^2 \gg 1, \quad (Re\,Fr^2)^{\frac{1}{2}} \ll 1.$$

Here $Re \equiv ch/\nu$, $Fr \equiv c/Nh$ and h is the half-thickness of an obstacle moving with transverse velocity c in a fluid of molecular viscosity ν and buoyancy frequency $N\,(\equiv [-g\rho_0^{-1}d\rho/dz]^{\frac{1}{2}})$. The dynamics of this flow are a balance between viscous and buoyancy forces. Browand & Winant also confirmed by experiment several aspects of the theory. A feature of the theory and experiments was the observation of an almost stagnant slug of fluid being pushed ahead of the obstacle with alternating jets above and below this slug in the environment. Janowitz (1974) has resolved the differences between his (1968, 1971) and Graebel's downstream predictions (non-diffusive fluid, shear layers) and those of Freund & Meyer (1972) (diffusive fluid, stagnant slug).

Maxworthy (1972) has invoked the low Reynolds number theory of Browand & Winant (1972) to interpret his experiments on the establishment of intrusions. He identified the slug of fluid observed to move with the obstacle in Browand & Winant's work with the intrusion from his source into a stratified tank. Using conservation of volume he predicted that the length of the intrusion would increase as $t^{\frac{2}{3}}$ and the thickness near the source as $t^{\frac{1}{3}}$. He confirmed the former prediction by laboratory experiment for low source flow rates but at higher rates the small source used caused so much mixing that the interpretation of results was ambiguous.

Only Foster & Saffman (1970) have considered in detail the effect that finite lateral extent has on the motions when an obstacle moves slowly and transversely in a stratified fluid. If a characteristic depth of the stratified region is H, it may be shown that the maximum velocity of disturbances which move upstream of the obstacle is $c_g = NH/\pi$ (see appendix). Since $c_g > c$, even for the high Reynolds number intrusions of prime interest here, it follows that almost from the start the obstacle is moving into fluid modified by prior disturbances. While this is only of conceptual interest to the formulations involving a viscous-dominated infinite stratified environment with steady flow fields about an obstacle, it is essential to an understanding of a Foster & Saffman result: that the upstream disturbances from the obstacle interact with each other and the end wall to establish shear layers which transfer fluid from in front of to behind the obstacle, thereby modifying the upstream stratification. They in effect showed that the stratification of the fluid in front of, and bounded vertically by, the obstacle decreases with increasing lateral displacement of the body until the body reaches the end wall, whereupon the fluid 'in front of' the obstacle has become homogeneous.

At high Reynolds numbers the viscosity–buoyancy dynamic balance may be expected to give way to an inertia–buoyancy balance for obstacle and intrusion behaviour in a stratified fluid. No such theoretical treatment has yet emerged however.

The complementary problem of the establishment of selective withdrawal

from a stratified reservoir has been the subject of an extensive study by Pao & Kao (1974). While the present problem is distinctly different, it does exhibit the same far-field, large time behaviour as the withdrawal problem: a series of forward-propagating disturbances centred about the level of the source or sink. The appendix derives this result for a source in a horizontal channel.

Zuluaga-Angel, Darden & Fischer (1972) have reported laboratory experiments on the present problem at Reynolds numbers almost as large as those achieved here. They, like Maxworthy (1972), used an approximation to a line source so the source fluid underwent an internal hydraulic jump on entering the tank. This caused considerable mixing – an object of their study – and resulted in secondary layers and much forward disturbance. They observed the length of intrusion to increase as $t^{\frac{3}{4}}$.

4. Experimental results and observations

The photographs in figure 1 (plate 1) show that intrusions into a continuously stratified fluid have a smooth pointed nose with no noticeable waviness: this confirms a speculation by Wilkinson & Wood (1972). The displacement of the environmental isopycnals results in an increase in the potential energy of the flow. This serves the same purpose as the breaking head wave of homogeneous gravity currents in balancing the driving pressure force.

If for the present the experimental tank, of depth $2H$, may be regarded as semi-infinite in length, dimensional analysis gives for the velocity of the nose of the rapid intrusion

$$c = \dot{q}^{\frac{1}{3}} N^{\frac{1}{3}} \,\mathrm{fn}\,(Re, \tau, \phi) \tag{4.1a}$$

and for the half-thickness measured in the vicinity of the source

$$h = \dot{q}^{\frac{1}{3}} N^{-\frac{1}{3}} \,\mathrm{gn}\,(Re, \tau, \phi). \tag{4.1b}$$

Here $Re \equiv \dot{q}/\nu$ is the characteristic intrusion Reynolds number based on the source volume flux $\dot{q}$ per unit breadth, $\tau \equiv Nt$ is the buoyancy time variable, and $\phi \equiv h/H$ is the depth ratio, defined in terms of h for convenience. Figure 2 defines the intrusion geometry.

The range of variation of the groups in relations (4.1) that could be covered in the laboratory experiments was limited by technical constraints. In particular the depth ratio ϕ varied little from a value of 0·15 and the maximum Re achievable without significant entrainment was about 500. The following definable stages in intrusion behaviour were noted by monitoring the intrusion thickness near the source for sufficiently high Reynolds numbers (viz. $\gtrsim 100$).

(i) An adjustment stage in which the intrusion flow was established. The time required to complete this stage was of order $\tau = 30$. It was often characterized by a slight transient temporal increase in thickness at higher Reynolds numbers, presumably because convective accelerations were more important then.

(ii) A quasi-steady stage in which h changed imperceptibly with time and the bulk of the flow moved as a slug without changes in nose form. This implies constant nose velocity, and is confirmed in figure 3.

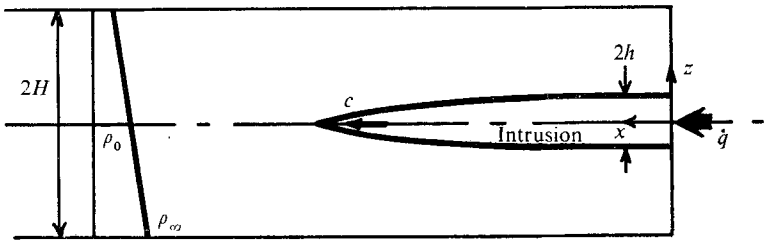

FIGURE 2. Sketch of the idealized intrusion based on figure 1.

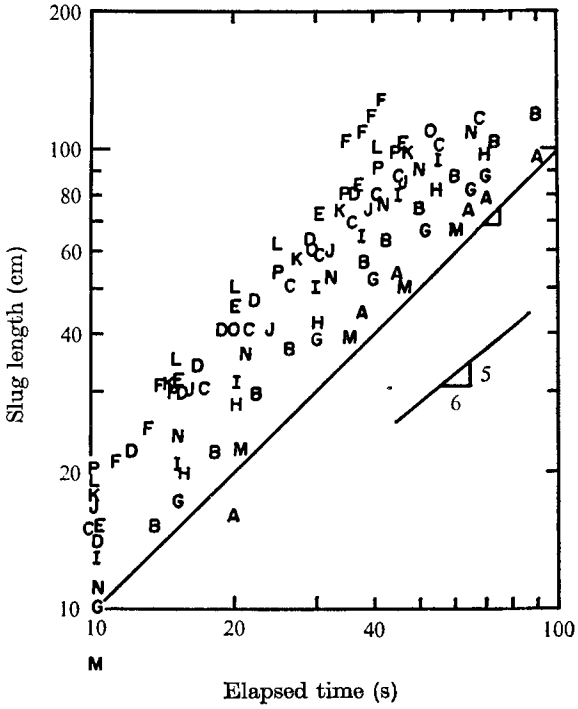

FIGURE 3. Intrusion slug length *vs.* elapsed time around stage (ii). The data symbols relate to different experiments.

	A	B	C	D	E	F	G	H	I
Re	72	110	142	180	183	225	101	116	148
N^2	14·3	12·3	14·5	11·5	15·5	12·9	6·65	6·65	7·0

	J	K	L	M	N	O	P
Re	181	224	255	86	159	208	257
N^2	6·61	6·52	7·29	3·81	3·09	3·51	3·75

(iii) A final stage where viscous stresses, or the end of the tank or both, noticeably slowed down the intrusion, causing its thickness to increase.

If the flow Reynolds number was too low then no definable stage (ii) was observed; the flow increased in thickness at all times, possibly tending to the particular time-dependent behaviour studied by Maxworthy (1972). It is stage (ii), where quasi-steady flow existed, which is of most dynamical interest here.

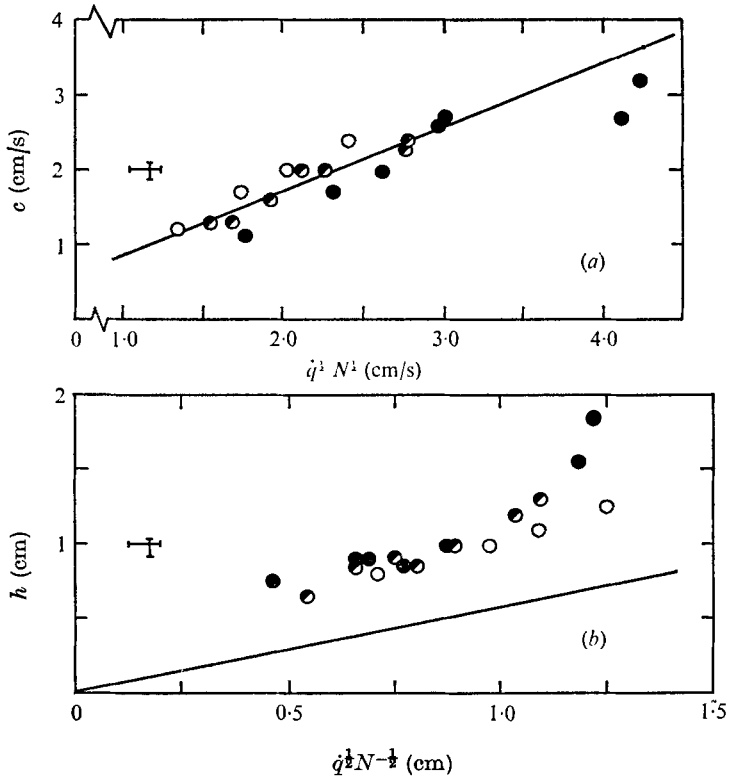

FIGURE 4. (*a*) Intrusion nose velocity, and (*b*) layer half-thickness as functions of source volume flux and environmental stratification. The flux $\dot{q}$ used in the figures is the observed flux computed from velocity and thickness readings. It differed from the input flux by about 5%, mainly because of uncertainties in reading, three-dimensional effects and a little entrainment near the source. The theoretical lines come from the hydraulic model of §5. Typical error bars for the data are indicated. ○, $N^2 = 3{\cdot}5$; ◐, $N^2 = 7{\cdot}0$; ●, $N^2 = 14$.

From figure 3, the intrusion length is proportional to time for practically all of the runs reported. There is no evidence of a $t^{\frac{5}{8}}$ dependence as found by Maxworthy (1972) at lower Reynolds numbers. For stage (ii), then, since ϕ changed but little between experiments and the Reynolds numbers were large, relations (4.1) should reduce to

$$c \propto \dot{q}^{\frac{1}{3}} N^{\frac{1}{3}}, \quad h \propto \dot{q}^{\frac{1}{2}} N^{-\frac{1}{2}}. \tag{4.2a, b}$$

The results for all experiments which had a well-defined second stage are presented in figure 4 as a test of relations (4.2). The data correlate well but there is systematic departure from universal relations when the data are ordered with respect to N^2. Very little dependence on Reynolds number is discernible in the data when correlated by (4.2). These correlations will be considered further after other results have been mentioned.

Figure 5 (plate 1) shows strong influence ahead of the nose, centred about the level of the intrusion. A velocity plot, figure 6, at a vertical section through the

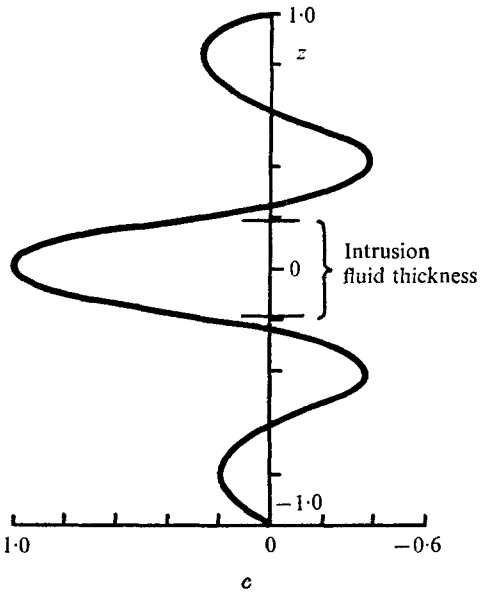

FIGURE 6. Normalized horizontal velocity at $x/L = 0{\cdot}44$ (L is the length of the tank) through the intrusion at a later time during the run in figure 5. The alternating jetting is characteristic of similar stratified flows. $\dot{q} = 3{\cdot}0$ cm^2/s, $N^2 = 6{\cdot}5$ s^{-2}.

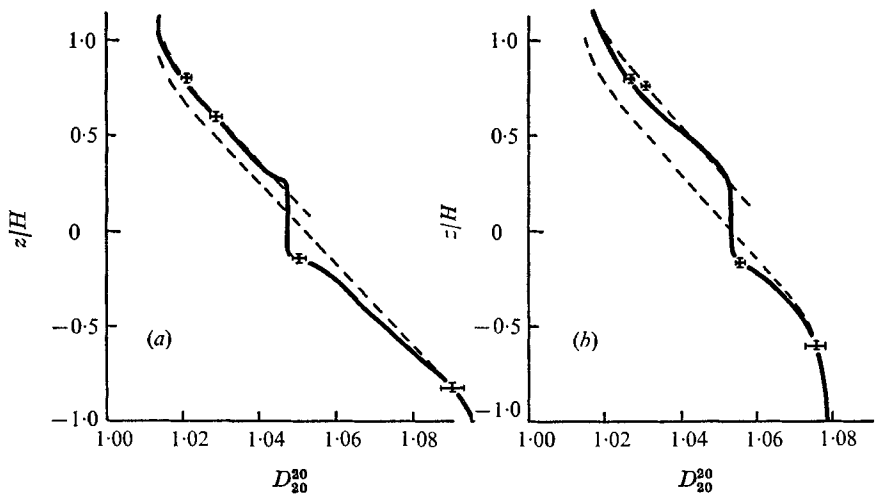

FIGURE 7. Specific gravity D_{20}^{20} *vs.* environmental depth at a section $x/L = 0{\cdot}16$ from the source. – – – –, initial; ———, well after the passage of the nose of the intrusion. The upper dashed line is the initial profile displaced to correspond to the increased fluid depth at the time the second profile was taken. (*a*) $\dot{q} = 1{\cdot}45$ cm^2/s, $N^2 = 6{\cdot}65$ s^{-2}. (*b*) $\dot{q} = 3{\cdot}0$ cm^2/s, $N^2 = 6{\cdot}52$ s^{-2}.

intrusion shows more clearly the alternating jets above and below it which are also visible in figure 5.

Vertical conductivity traverses through the intrusion resulted in the (slightly smoothed) examples in figure 7. It can be seen particularly in figure 7(*a*) that the straining of the isopycnal field due to the intrusion occurs primarily immediately above and below the intrusion. The straining is achieved by the jetting in the environment and is visible in the right-hand dye streaks in figure 5. The asymmetry about the intrusion level in figure 7 is probably due to the difference in tank top and bottom boundary conditions. Fluid below the intrusion is relatively quiescent but that above is all rising to increase the free-surface elevation as source fluid is added.

The systematic departures from universal curves of the correlations in figure 4 and the strong forward-propagating effects observable in figure 5 suggest that the latter may be interacting with the far end wall of the tank in a manner like that found by Foster & Saffman (1970): in particular to modify the initial stratification as mentioned above (§3). A qualitative observation in the experiments supports this. After a certain time during an experiment the source would be shut off. The intrusion would continue to penetrate for several seconds and then halt. When observed some 12–15 h later, the intrusion would be in approximately the same position. This could only occur if the remaining ambient fluid in front of the intrusion and bounded by the intrusion thickness had become practically homogeneous during the penetration.

5. A simplified hydraulic intrusion model

It has been shown in §4 that a rapid intrusion at constant volume flux into a stably stratified environment reaches a quasi-steady state in which inertia forces and buoyancy forces balance. This suggests the following approximate hydraulic model of the intrusion, motivated by the similarity the flow has to conventional gravity currents. There are important over-simplifications required of the approach.

Axes are taken moving with the (supposed steady) nose velocity c of the intrusion. Deviations from this velocity within the intrusion are ignored, and the flow is confined to a channel of depth $2H$. The plane $z = 0$ is a plane of symmetry. Figure 8 is a sketch of conditions in the new co-ordinate system.

The equation of motion on the plane $z = 0$ for inviscid Boussinesq fluid is

$$\frac{\partial u}{\partial t} + \frac{\partial}{\partial x}\left(\int_0 \frac{dp}{\rho_0} + \tfrac{1}{2}u^2\right) = 0. \tag{5.1}$$

Here u is the horizontal fluid velocity, p the pressure and ρ_0 the density at $z = 0$. Equation (5.1) is to be integrated along $z = 0$ from $x = G$ to $x = E$. Far enough upstream, at point E, no propagating disturbances have yet arrived, so the initial hydrostatic conditions prevail and the relative flow velocity is steady, i.e. $u = -c$.

The downstream point G in figure 8 is positioned at $x \ll 0$, where the intrusion is of uniform thickness, so hydrostatic conditions are again approached. Above

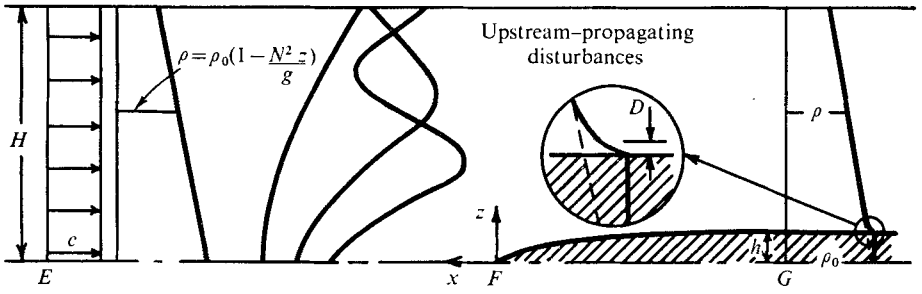

FIGURE 8. Assumed environmental conditions relative to the intrusion for the hydraulic model.

G it is assumed that the straining of the environmental density stratification is concentrated into a region in the vicinity of the intruding fluid. The length scale of the disturbance is D (figure 8), and $D \ll H$. The density traverses shown in figure 7 indicate that this is a reasonable assumption in the experiments.† A fair approximation to the environmental density anomaly $d(z)$ is

$$d(z) = \begin{cases} d(h)\exp[-(z-h)/D] & \text{for } z \geqslant h, \\ 0 & \text{for } z < h, \end{cases} \tag{5.2}$$

where

$$d(h) = \rho_0 N^2 h/g. \tag{5.3}$$

Integrating (5.1) along the x axis between G and E gives

$$\tfrac{1}{2}c^2 = \frac{1}{\rho_0}\int_0^H [\rho(z)+d(z)]\,g\,dz\Big|_G - \frac{1}{\rho_0}\int_0^H \rho(z)\,g\,dz\Big|_E - \int_G^E \frac{\partial u}{\partial t}\,dx,$$

which, in view of the assumptions made about the sections $x = G, E$, gives

$$\tfrac{1}{2}c^2 = \tfrac{1}{2}N^2h^2 + N^2Dh - \int_G^E \frac{\partial u}{\partial t}\,dx. \tag{5.4}$$

Now the only unsteady regions in the model flow are in the vicinity of the fronts of the columnar wave disturbances (discussed in the appendix) which are able to propagate upstream faster than the relative flow velocity c. There are M such wave fronts, given by the condition that

$$c - c_m < 0, \quad 1 \leqslant m \leqslant M. \tag{5.5}$$

c_m is the group velocity of the mth mode [equation (A 5)], so

$$M = \text{integer part}\,(NH/\pi c). \tag{5.6}$$

It follows from the discussion in the appendix of the properties of the columnar waves that the contribution to the integral in (5.4) from the mth unsteady front for large times is

$$\int \frac{\partial u_m}{\partial t}\,dx \simeq -\,u_m \frac{NH}{m\pi}. \tag{5.7}$$

† The velocity jetting and departure from undisturbed density stratification in the environment above and below the intrusion are important. They render an application of Bernoulli's equation along the intrusion surface invalid; cf. the gravity current (Benjamin 1968).

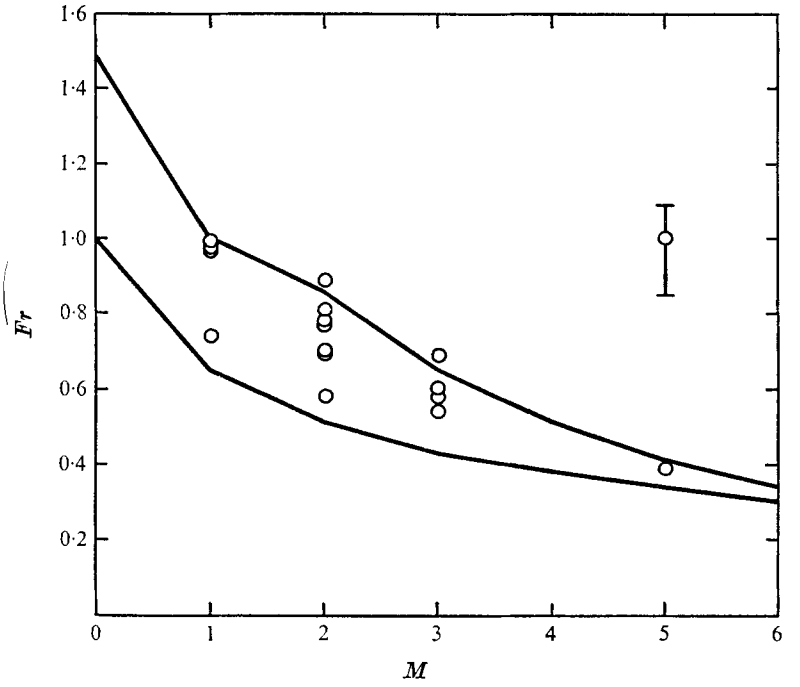

FIGURE 9. Internal Froude number c/Nh as a function of M, the number of forward-propagating columnar modes from (5.6). The curves are upper and lower bounds from the simplified hydraulic model. Typical error bars on Fr are indicated for the data points.

Here u_m is the amplitude of the disturbance velocity far upstream due to the mth mode.

The problem of obtaining the disturbance amplitudes is simplified in the model because the advective and inertial terms are small, although the horizontal velocities behind the fronts may be large. The linearized Oseen problem for the channel can be solved readily. If the obstacle in figure 8 is replaced by a source of strength $q\,(=ch)$ in an initially uniform stream of velocity c, Wong & Kao (1970) have shown that for large times disturbances penetrate far upstream and contribute

$$u_m \cos\frac{m\pi z}{H} = -\frac{ch\cos(m\pi z/H)}{H(1-m\pi c/NH)}, \quad 1 \leqslant m \leqslant M, \tag{5.8}$$

to the velocity field there. The Mth mode has the largest amplitude but the lowest wave speed.

Substitution of (5.7) and (5.8) into (5.4) gives

$$Fr^2 = 1 + \frac{2D}{h} - \sum_{m=1}^{M} \frac{2Fr}{m\pi(1-Fr\phi)}, \tag{5.9}$$

where $Fr = c/Nh$ and ϕ is the depth ratio h/H.

Within the restrictions of the model, two limits on the predicted internal Froude number may be obtained from (5.9) and compared with the experiments.

A lower bound on Fr

It is assumed that the disturbance to the environmental density gradient above and below the intrusion at $x = G$ is negligible in so far as it contributes to the pressure there. That is $D = 0$. Further, the experimental tank is assumed to be infinitely long so that all M disturbance fronts are in the fluid at large times. Then (lower bound)

$$Fr^2 = 1 - \sum_{m=1}^{M} \frac{2Fr}{m\pi(1 - m\pi Fr\phi)}. \tag{5.10}$$

If the flow were steady the predicted Fr would be unity, but as the permitted number of forward-propagating modes increases (M increases), Fr decreases from unity. Energy is propagated ahead of the intrusion to modify the environment, so the intrusion travels relatively more slowly for increased M.

Figure 9 compares Fr calculated from (5.10) using $\phi = 0{\cdot}15$, the average value for the experiments reported in §4, with the internal Froude numbers obtained from the experiments. M is obtained from (5.6). Equation (5.10) is a good lower bound.

An upper bound on Fr

First consider the flow to be steady everywhere, so that (5.9) becomes

$$Fr^2 = 1 + 2D/h. \tag{5.11}$$

Then the change in the kinetic energy of the steady horizontal flow between $x = E$ and $x = G$ in figure 8 must equal the increase in the potential energy of the flow resulting from the rising of the isopycnals to clear the obstacle. The resulting expression is

$$\tfrac{1}{2}hc^2/(1-\phi) = \tfrac{1}{3}N^2h^2 + N^2h(D^2 + Dh),$$

or

$$\tfrac{1}{2}Fr^2/(1-\phi) = \tfrac{1}{3} + (1 + D/H)\,D/h. \tag{5.12}$$

Solution of (5.11) and (5.12) for Fr and D/h with $\phi = 0{\cdot}15$ gives

$$Fr \simeq 1{\cdot}48, \quad D/h \simeq 0{\cdot}6. \tag{5.13), (5.14}$$

If $\phi \to 0$, $Fr^2 \sim 1 + (\frac{2}{3})^{\frac{1}{2}}$ and $D/h \sim (\frac{1}{6})^{\frac{1}{2}}$.

The value (5.13) gives a crude upper bound on Fr. More realistic are the following circumstances. Because the experimental tank is of finite length, the forward-propagating disturbances will reach the far end and be reflected. On reflexion the mth mode cancels itself out. Thus for sufficiently large times all contributions to (5.7) will be destroyed by reflexion except for the Mth mode, which is travelling only slightly faster than the intrusion velocity c.

An upper bound on Fr is then obtained by permitting only the Mth front to be present in the flow. From (5.9), using D/h from (5.14) (upper bound),

$$Fr^2 = 2{\cdot}2 - \frac{2Fr}{M\pi(1 - M\pi Fr\phi)}. \tag{5.15}$$

Because in this limit the number of fronts upstream of the intrusion is not decreasing with time through reflexion at the end wall, the Froude number

observed in a finite tank would be time independent once the flow was established. This upper limit is therefore more likely to be that approached by an experimental intrusion than is the lower bound.

Figure 9 illustrates (5.15) for $\phi = 0{\cdot}15$. Considering the uncertainty in experimentally determining the internal Froude numbers the data and the upper bound (5.15) compare very favourably.

The upper bound (5.13) expressed in terms of c and h is also plotted in figure 4. For the nose velocity of the intrusion it is an upper bound and for the intrusion half-thickness it is a lower bound. It can be seen that the intrusion thickness is more strongly affected by the columnar waves than the velocity of intrusion. The additional systematic dependences of N^2 found in figure 4 are also explicable in terms of the presence of columnar waves. The larger N is, the larger is M from (5.6) and so the smaller is Fr from (5.15). Then, for a given $\dot{q}^{\frac{1}{2}}N^{\frac{1}{2}}$, c decreases as N increases, and for fixed $\dot{q}^{\frac{1}{2}}N^{-\frac{1}{2}}$, h increases as N increases.

6. Conclusion

At sufficiently high Reynolds numbers the intrusion of a homogeneous fluid into a stably stratified environment at its equilibrium level is, from the preliminary experiments reported, dynamically self-determined after an initial transient period. An inertia–buoyancy balance is observed in which the internal Froude number based on the intrusion is of order unity. The internal Froude number decreases with an increase in the number of permissible forward-propagating columnar waves.

A hydraulic model of the experimental arrangement is able to predict upper and lower bounds on the internal Froude numbers observed. Even though the model assumes vertical symmetry about the centre-line of the intrusion, the predicted bounds compare very well with the results of the experiments. It is inferred that the end walls of the tank and the columnar waves present play a crucial role in the experiments.

The basis of this paper is part of the writer's Ph.D. dissertation (Manins 1973). A debt of sincere gratitude for inspiration and example is owed Dr J. Stewart Turner. The receipt of a Commonwealth Scholarship is also gratefully acknowledged.

Appendix. The propagation of disturbances

The nature of the propagation of disturbances ahead of a rapid intrusion may be examined by considering a simplified linear problem.

A line source $2\dot{q}\delta(x)\,\delta(z)$ is turned on at time $t = 0$ in an infinite channel of depth $2H$. $\delta(x)$ is Dirac's delta function. The inviscid, non-diffusive, linearly stratified fluid which fills the channel is initially at rest; inertia effects are ignored; only the region $x > 0$ is considered. Figure 2 defines the co-ordinate

system used. The equations of motion in the Boussinesq approximation are

$$\left.\begin{aligned} \rho_0 \frac{\partial u}{\partial t} &= -\frac{\partial p'}{\partial x}, \quad \rho_0 \frac{\partial \omega}{\partial t} = -\frac{\partial p'}{\partial z} - \rho' g, \\ \frac{\partial \rho}{\partial t} &= -\omega \frac{N^2}{g} = 0, \quad \frac{\partial u}{\partial x} + \frac{\partial \omega}{\partial z} = 2\dot{q}\delta(x)\,\delta(z)\,H(t). \end{aligned}\right\} \tag{A 1}$$

Here $H(t) = 1, 0$ for $t \gtrless 0$; ρ' and p' are departures in density and pressure from the initial hydrostatic state. Then, with $\partial u/\partial z = 0$ on $z = \pm H$, the solution for the horizontal velocity field for $x > 0$ is

$$u(x,z,t) = \frac{\dot{q}}{H}\left[\tfrac{1}{2} + \sum_{m=1}^{\infty} \cos\frac{m\pi z}{H}\frac{1}{2\pi i}\int_{\epsilon-i\infty}^{\epsilon+i\infty} \frac{1}{p}\exp\left(pt - m\pi x/\alpha H\right) dp\right], \tag{A 2}$$

with $\epsilon > 0$ and $\alpha^2 = 1 + N^2/p^2$.

The integral in (A 2)

$$I(mx,t) = \frac{1}{2\pi i}\int_{\epsilon-i\infty}^{\epsilon+i\infty} \frac{1}{p}\exp\left(pt - m\pi x/\alpha H\right) dp \tag{A 3}$$

has been studied in a similar context by McEwan & Baines (1974) in the large time limit. As a first approximation it reduces for large x to

$$I(mx,t) \sim \exp\left(-m\pi x/NHt\right). \tag{A 4}$$

The result (A 4) shows that the various modes of disturbance are columnar waves of zero frequency: they propagate away from the source in the form of horizontal jet-like columns with velocities

$$c_m = NH/m\pi \quad (m = 1, 2, \ldots). \tag{A 5}$$

The position of the front of the disturbance for mode m is given by

$$x = HNt/m\pi + 3^{\frac{1}{3}}BH(Nt)^{\frac{1}{3}}/2m\pi, \tag{A 6}$$

where $B = O(1)$. The integral I grows practically linearly from very near zero to very near unity within the range $-1{\cdot}2 < B < 1{\cdot}0$.

Thus the nature of the disturbances which propagate forwards from a source-like disturbance in a stratified fluid is approximately as follows. At large times a set of columnar waves of zero frequency is to be found far ahead of the source. The waves travel at the group velocities given by (A 5) behind a front of width given by the second term of (A 6), i.e. $O(H(Nt)^{\frac{1}{3}}/m)$. The fluid velocity for the mth mode grows practically linearly from very near zero to very near its maximum value within the frontal region. The flow is steady back to the front of the $(m-1)$th mode, where there is another unsteady region.

REFERENCES

BENJAMIN, T. B. 1968 Gravity currents and related phenomena. *J. Fluid Mech.* **31**, 209–248.

BROWAND, F. K. & WINANT, C. D. 1972 Blocking ahead of a cylinder moving in a stratified fluid: an experiment. *Geophys. Fluid Dyn.* **4**, 29–53.

FORTUIN, J. M. H. 1960 Theory and application of two supplementary methods of constructing density gradient columns. *J. Polymer Sci.* **44**, 505–515.

FOSTER, M. R. & SAFFMAN, P. G. 1970 The drag of a body moving transversely in a confined stratified fluid. *J. Fluid Mech.* **43**, 407–418.

FREUND, D. D. & MEYER, R. E. 1972 On the mechanism of blocking in a stratified fluid. *J. Fluid Mech.* **54**, 719–744.

GRAEBEL, W. P. 1969 On the slow motion of bodies in stratified and rotating fluids. *Quart. J. Mech. Appl. Math.* **22**, 39–54.

JANOWITZ, G. S. 1968 On wakes in stratified fluids. *J. Fluid Mech.* **33**, 417–432.

JANOWITZ, G. S. 1971 The slow transverse motion of a flat plate through a non-diffusive stratified fluid. *J. Fluid Mech.* **47**, 171–181.

JANOWITZ, G. S. 1974 Blocking in slow stratified flows. *J. Geophys. Res.* **79**, 1265–1268.

MCEWAN, A. D. & BAINES, P. G. 1974 Shear fronts and an experimental stratified shear flow. *J. Fluid Mech.* **63**, 257–272.

MANINS, P. C. 1973 Confined convective flows. Ph.D thesis, University of Cambridge.

MAXWORTHY, T. 1972 Experimental and theoretical studies of horizontal jets in a stratified fluid. *IAHR/AIRH Int. Symp. on Stratified Flows, Novosibirsk*, communication 17.

MIED, R. P. & MERCERET, F. J. 1968 The construction of a simple conductivity probe. *Johns Hopkins University, Dept. Mech. Rep.*

PAO, H.-P. & KAO, T. W. 1974 Dynamics of establishment of selective withdrawal of a stratified fluid from a line sink. Part 1. Theory. *J. Fluid Mech.* **65**, 657–688.

WILKINSON, D. L. & WOOD, I. R. 1972 Some observations on the motion of the head of a density current. *J. Hydraul. Res.* **10**, 305–324.

WONG, K. K. & KAO, T. W. 1970 Stratified flow over extended obstacles and its application to topographical effect on vertical wind shear. *J. Atmos. Sci.* **27**, 884–889.

ZULUAGA-ANGEL, A., DARDEN, R. B. & FISCHER, H. B. 1972 Flow into a stratified reservoir. *U.S. Environ. Protection Agency Wash. Rep.* EPA-R2-72-037.

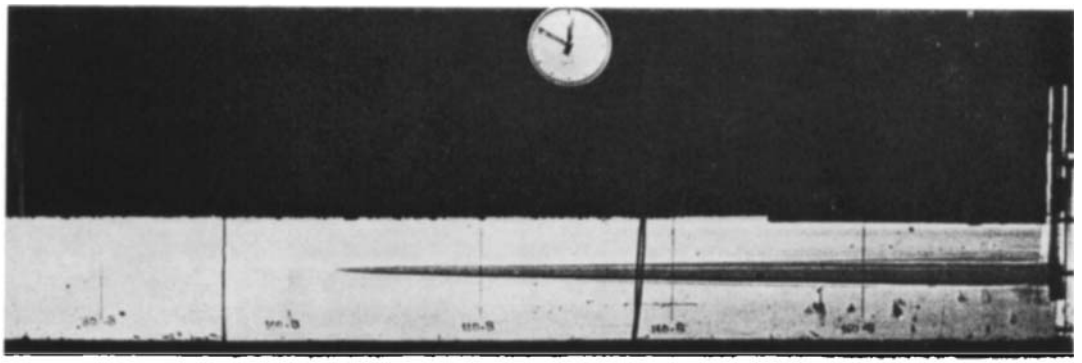

(*a*)

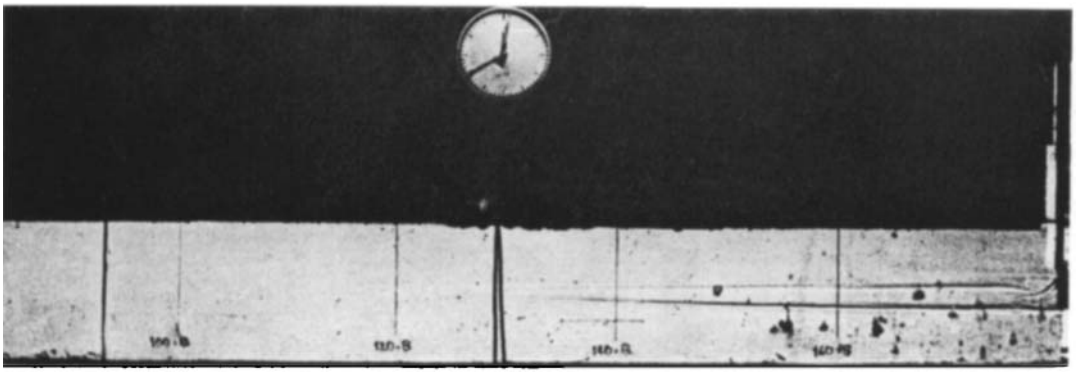

(*b*)

FIGURE 1. Photographs of shadowgraphs from two intrusion experiments. The clock indicates elapsed time from 00–00 h. The intrusion source is at the extreme right of the tank of stratified salt water, at approximately the mid-depth. (*a*) A small amount of dye has been added to the needle-like intrusion fluid. Note the smooth outline of the intrusion, the thickness of which near the source is not related to the vertical position and size of the source. (*b*) Similar to (*a*) but no dye is present. A different behaviour near the source is exhibited, again illustrating source-geometry independence.

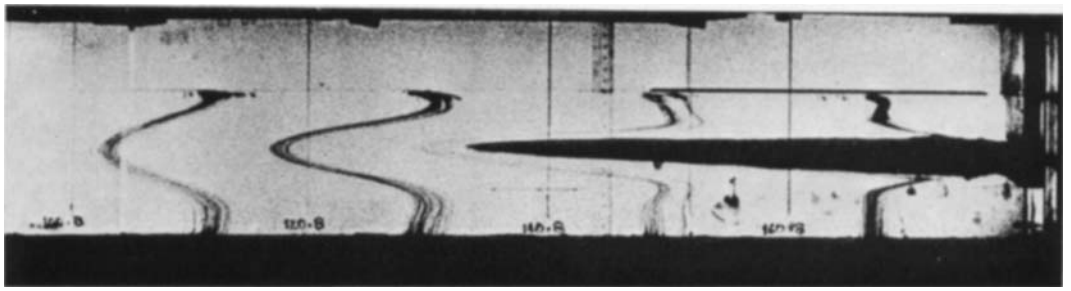

FIGURE 5. Dye-streak distortion from the vertical in the apparatus due to the intrusion, shortly after the start of a run.